Large Isospin Selection-Rule Violation in the $^{20}Ne(d,\alpha)^{18}F$ Reaction*

A. F. Hrejsa† and C. P. Browne
Department of Physics, University of Notre Dame, Notre Dame, Indiana 46556
(Received 27 November 1972)

Absolute differential cross sections were measured at 125° with $6 \leq E_d \leq 11$ MeV for the $^{20}Ne(d,\alpha)^{18}F$ reaction leading to the 1.70-, 2.10-, 2.52-, 3.06-, 3.13-, and 3.36-MeV states of ^{18}F and at 45° with $5 \leq E_d \leq 13$ MeV for the 2.52-, 3.06-, and 3.13-MeV states. Angular distributions were measured at 6.66, 7.29, 7.93, and 12.95 MeV for the 2.52-, 3.06-, 3.13-, 3.36-, and 4.12-MeV states and at the three lower energies for the 2.10-MeV state. Uncertainties for the isolated states are 3.4%; for the 3.13-MeV state, 5.7%; and for the 3.06-MeV state, 5.7 to 20.2%. The ratio of the cross section for the forbidden reaction to the 3.06, 2^+, $T=1$ state to the cross sections for the other five ($T=0$) states ranges from 6 to 40% with an average of 21%. The reaction appears to proceed through the compound nucleus. The large violation is discussed in terms of mixing in the compound nucleus and final-state impurity.

I. INTRODUCTION

A number of measurements[1-9] have been made of (d, α) reactions proceeding to $T=1$ states in light nuclei, in violation of the isospin selection rule. As data have accumulated some patterns have begun to appear in the results. In most cases, the excitation of the $T=1$ states is a few percent of the isospin-allowed excitation of neighboring $T=0$ states. One remarkable exception[4] is the excitation of the 16.6- and 16.8-MeV states in ^8Be where these final states evidently do not have a well-defined value of T. Another apparently exceptional case was found by Matous and Browne[10] in the $^{20}Ne(d, \alpha)^{18}F$ reaction leading to the second $T=1$ state in ^{18}F. Here the yield to the $T=1$ state was found to be of the order of 40 percent of the yield to a neighboring state. At the time this work was done, the spins and parities of the states were not established and it was thought that the situation might be similar to ^8Be where two states of identical J^π, but different T, which would lie very close to each other in the absence of the Coulomb force, actually have mixed T values and a somewhat greater spacing.[11]

We now know[12,13] that in ^{18}F there is no other 2^+ state close to the 2^+, $T=1$ state and hence a very large isospin impurity seems unlikely. The work of Matous and Browne was necessarily limited to the small bombarding-energy range of 3.5 to 4.5 MeV. From experience with other (d, α) reactions we expect compound-nucleus formation to dominate in this region and to find considerable isospin mixing in the compound nucleus. We thought it would be interesting and informative to extend the measurements of the forbidden (d, α) yield to higher deuteron energies. As the deuteron energy is raised we expect the cross section for the $T=1$ state to decrease because the reaction will become more direct and there will be less time for Coulomb mixing in the compound nucleus. Or more precisely, the average level width will become greater than the Coulomb matrix element $\langle H_C \rangle$ and the dynamic criterion for isospin conservation will become valid. With the availability of the Notre Dame FN tandem accelerator we could try to observe the onset of this dynamic criterion.

We wished to compare cross sections to $T=1$ and $T=0$ states in ^{18}F and especially to compare states of differing isospin but the same J^π since these may be formed in the same way. Such comparisons should shed light on the mechanism for formation of the $T=1$ states. The work was concentrated on the 3.060-MeV, $J^\pi=2^+$, $T=1$ state in ^{18}F. The fact that this state is not 0^+ reduces the complication of angular momentum and parity selection rules,[14] present in so many of the (d, α) studies involving 0^+ initial and final states. Our results are compared with those from other (d, α) reactions to elucidate trends in the isospin-forbidden reaction.

Yield curves were measured at 125° lab for six excited states and for three of these states also at 45° lab. The energy ranged from 5 to 13 MeV. Angular distributions were taken for six states at four deuteron energies between 6.6 and 8.0 MeV and for five of these states also at 12.95 MeV. The cross-section measurements are absolute. We compare the results for the 3.060, 2^+, 1 state with the results for all the other states which were resolved. It was not possible to resolve the 3.836, 2^+, 0 state from the 3.787-MeV state so these states are not included, but the other 2^+ level at 2.524 MeV was measured.

II. EXPERIMENTAL PROCEDURE

The α particles from the $^{20}Ne(d, \alpha)^{18}F$ reaction were analyzed with our 50-cm broad-range spec-

trograph and recorded with nuclear track plates or a position-sensitive proportional counter along the focal surface. We were able to count many more particles with this counter[15] than would have been possible with plates alone and thus greatly reduce statistical uncertainties as well as shorten data taking by many months. The counter has a 50.8-cm-long high-resistance center fiber mounted in a shallow rectangular cavity. The difference in arrival time of a pulse at the two ends of the fiber provides position information and a pulse from the insulated body of the counter gives energy loss and hence particle identification. Charge-sensitive preamps are used and the time difference is converted to a pulse height. We find that the calibration of position pulse vs trajectory radius remains constant in shape, but does shift slightly each time the electronics is set up.

All angular-distribution runs were normalized to the counts recorded by one or both of two surface-barrier detectors mounted at −45 and −135° in the target chamber. This normalization compensated for any fluctuation in target density or charge integration.

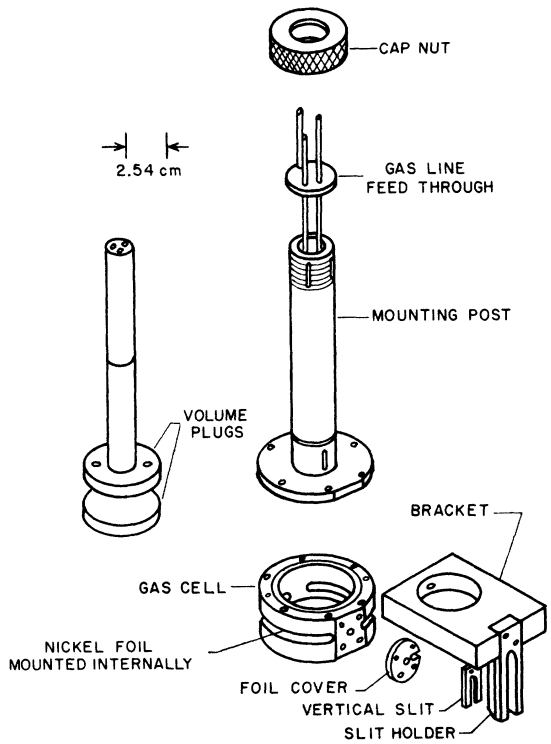

FIG. 1. Exploded view of gas target cell. The entire cell rotates in a bearing in the target-chamber lid so that the exit window and slit always point toward the spectrograph.

A cell was required to contain the target gas and one of the most difficult problems was to reduce the energy straggle of the α particles enough to resolve the 3.060- and 3.135-MeV states. A cell was designed (see Fig. 1) that rotates with the spectrograph so that a small plastic window of only 5.16 mm diam always points toward the spectrograph. Because the exit window is so small and because it does not have to sustain the beam, it can be made very thin. Thus the reaction α particles, with their high specific energy loss, lose a minimum of energy and minimal straggling is introduced. The deuteron beam (which has a much lower specific energy loss) enters and leaves through a thin nickel foil.

Many materials were tried for the exit windows including nickel, VYNS, Formvar, Collodian, Mylar of various thicknesses, stretched Mylar, and combinations of these. In all cases where mechanical strength was sufficient, the measured energy straggle was too high. Success was achieved with the plastic,[16] Parylene C. A 0.15-μm window held only 15 Torr but 0.65-μm windows held up to 76 Torr for at least 24 h. The energy loss and straggle of the latter were acceptable and they were used for most runs. A 127-μm-thick nickel foil[17] was wrapped around the inside of the cell to cover the beam slot. This foil was layed down with a Teflon roller. Both the nickel and Parylene foils were sealed with Celvaseal cement.[18] For a complete description of cell windows, energy-straggle calculations, and measurements, see Ref. 19.

The active depth of target gas was defined in the horizontal plane by a vertical slit outside the exit window of the cell and by the focal-surface slits of the spectrograph. The angular acceptance in the horizontal plane, which determins the kinematic energy spread, is fixed by these slits and by the angular spread of the beam. The angular spread was set by an adjustable slit 168 cm upstream and a fixed slit immediately ahead of the cell. Slit openings were carefully chosen to minimize the contribution of the kinematic spread to the total energy spread. After much experimentation[19] normal operating conditions of 38- to 50-Torr gas pressure, 7.62-mm beam-defining slits, 2.38-mm cell slits, and a 1-cm focal-surface slit were chosen.

The target gas was either research-grade natural neon, filtered over liquid-nitrogen-cooled activated charcoal, or ^{20}Ne enriched to 99.96 mole %.[20] Gas pressure was measured with a manometer filled with Octoil S diffusion-pump oil. Constant pressure during a run was assured by monitoring the manometer. Nitrogen and oxygen contamination were found in the target gas when the oil mano-

meter and gas cell were first used. Running a beam through the gas cell for about two hours and then flushing and refilling with clean gas eliminated the problem for the remainder of any run. The target-chamber temperature was measured with a glass-mercury thermometer.

All quantities needed for determination of the absolute differential cross section were directly measured. We checked the accuracy of the measurements by observing proton-proton elastic scattering at 20° and 6.138 MeV, using hydrogen in the cell and the position-sensitive counter for recording. Ten runs were made with various slit settings and using different regions of the counter. This check led to remeasurement of the width of the exit slit. An error of 2.7% was found in the value being used and correction was made. Our result for the p-p cross section then agreed within the estimated error of 1.3% with the published value.[21]

III. DATA REDUCTION AND RESULTS

The center-of-mass cross section was derived from the observed number of counts in a group using the following formula:

$$\frac{d\sigma}{d\Omega} = \frac{\sin\theta_0 \, Y G(x, \theta_0)}{n N G_{00}},$$

where $d\sigma/d\Omega$ is the cross section, Y is the number of particles in the group (yield), θ_0 is the lab angle of observation, $G(x, \theta_0)$ is the lab-to-c.m. conversion factor,[22] G_{00} is the geometric factor of the gas-cell–spectrograph-slit system, n is the number of incident deuterons, and N is the number of target nuclei/cm^3. The geometric factor was calculated by the method of Silverstein,[23] with the realization that the distance to the focal-surface aperture of the broad-range spectrograph varies with the trajectory radius of the detected particle.

Since the 3.060- and 3.135-MeV states were not totally resolved in this experiment, a computer fit was made to extract the quantity Y for these groups. The code fitted the composite group under the assumption that both groups had the same half widths. The shape used for each group is two halves of a Gaussian where the low-energy half can be wider than the high-energy half. A linear

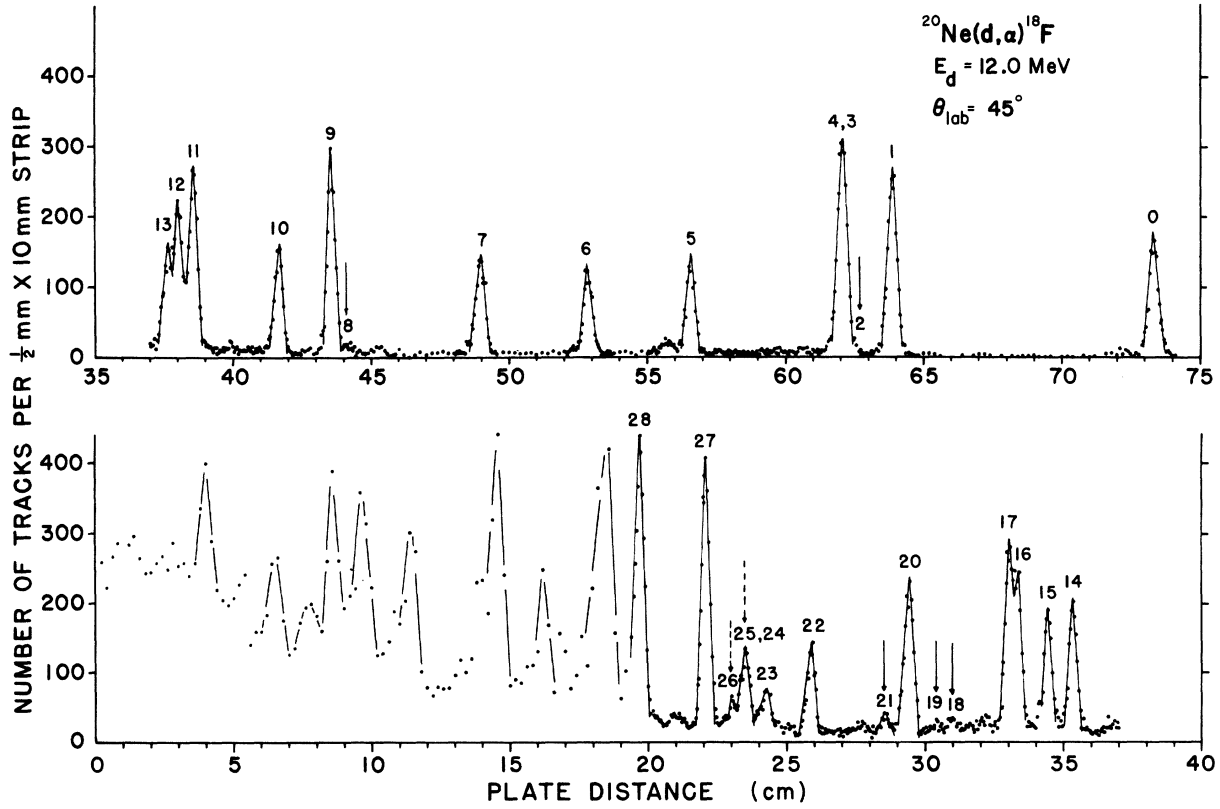

FIG. 2. Example of a ^{20}Ne$(d,\alpha)^{18}$F spectrum recorded on plates. Arrows point to $T=1$ states in ^{18}F below 6 MeV excitation. The states are numbered in order corresponding to the listing in Ref. 13. For this run the pressure was 15 Torr, exit window 0.15-μm Parylene C, and collected charge 5500 μC.

background was assumed. The code uses a variable metric minimization procedure written by Davidon[24] to minimize the χ^2 function and also corrects the input deuteron energy for losses suffered in reaching the center of the cell. The areas less background under the groups are then calculated, a correction is made for the change in solid angle of the spectrograph with position along the focal surface, and the center-of-mass differential cross section is computed. Corrections are made for energy losses of the outgoing particles and a Q value and center-of-mass angle are computed.

Figure 2 shows a spectrum taken with plates at $E_d = 12$ MeV and 45° lab angle. The arrows show positions of the known $T = 1$ states. Group 8 corresponds to the 3.060-MeV, $J^\pi = 2^+$, $T = 1$ state which was of major interest in this work. It is well resolved from the 3.135, 1^-, 0 state (group 9) in this case. Groups 18, 19, and 21 are the 4.650, 4^+, 1; 4.739, 0^+, 1; and 4.957, 2^+, 1 states. Groups 25 and 26 are the 5.606- and 5.674-MeV states. Both of these states have been assigned $J^\pi = 1^-$ with reasonable assurity[25] and the isospin is thought to be highly mixed. A recent tabulation[13] lists a state at 5.599 MeV, (4^+), 0. Our resolution with the gas cell was not sufficient to separate this from the 5.607-MeV group. The dashed arrows in Fig. 2 suggest the uncertainty in T assignments in this region. We did not attempt to analyze the spectrum above the 6.099-MeV state so no solid lines are shown in Fig. 2 beyond group 28. The majority of runs did not include groups 18 to 26 so only a few isolated points on a yield curve could have been obtained for the $T = 1$ states in this region. State number 2 lies too close to states 3 and 4 to be resolved with the gas cell.

Figure 3 shows a proportional-counter spectrum taken at $E_d = 6.66$ MeV and 30°. Fewer states are shown here because of the reduced detector length and the lower deuteron input energy (the dispersion of the spectrograph is larger). Here again the 3.060- and 3.135-MeV states are fairly well resolved.

Yield Curves

Yield curves were taken at 45 and 125°. The most complete data are for the 2.524-, 3.060-, and 3.135-MeV states. The 45° yield curves shown in Fig. 4 cover deuteron energies of 4.5

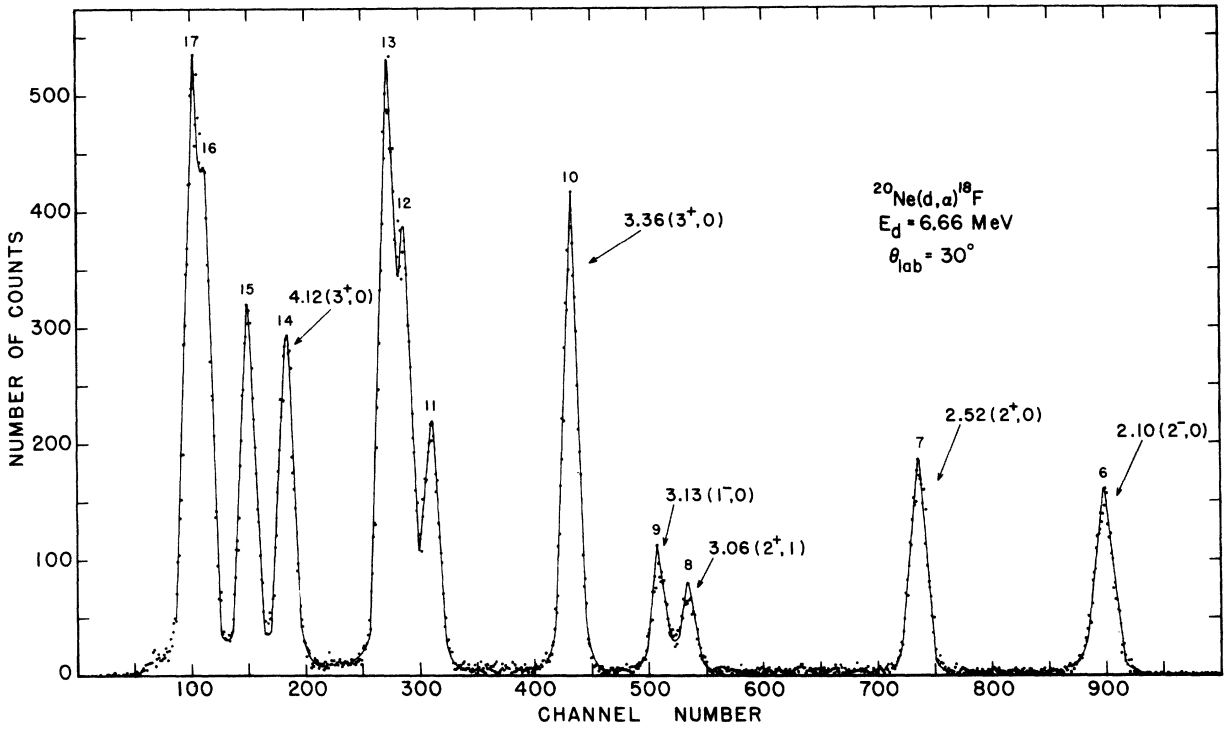

FIG. 3. Example of a $^{20}Ne(d,\alpha)^{18}F$ spectrum recorded with the position-sensitive proportional counter. The group numbers correspond to Fig. 2. Groups for which angular distributions were measured are labeled with excitation energy, J^π, and T. For this run the pressure was 38 Torr, exit window 0.65-μm Parylene C, and collected charge 1500 μC.

to 13 MeV whereas those taken at 125° and shown in Fig. 5 range from $E_d = 6.4$ to 10.5 MeV for these three states. Figure 6 shows yields of the 1.701-, 2.101-, and 3.357-MeV states at 125° from $E_d = 6.4$ to 10.5 MeV. The energy steps in the yield curve are large compared to the target stopping which was less than 10 keV for 10-MeV deuterons.

The plate data, which represent about half the data at 45°, were corrected for the natural abundance of ^{20}Ne in research-grade neon. It was still necessary to normalize to the proportional-counter data. The plate data are not completely consistent with the proportional-counter data because they were taken early in the experiment, before it was realized that some reaction particles were intercepted by too small an opening in the gas cell. Also at the time the plate data were taken the magnitude of the contaminant problem was unknown. The plate data were raised by a factor of 1.657 ± 0.091. This represents the average of six data points in three repeated runs. These six were the ones for which the input deuteron energy differed by no more than ±2 keV, the computer fits were good in terms of χ^2, and there was no hint of contaminant groups. An average of 23 data points from seven repeated runs where the input energy varied by as much as 33 keV gave a factor of 1.645 ± 0.16. It is felt that the six data points are more reliable because of the lower variation in input energy and therefore 1.657 was used to normalize the plate data to the absolute values from the proportional-counter runs.

Yield data were taken on plates at 45° lab angle up to $E_d = 16$ MeV but analysis for the 3.060- and 3.135-MeV states was impossible above 13 MeV because groups arising from the (d, α) reactions on ^{22}Ne and ^{14}N (which were of the same order of magnitude as the 3.060-MeV state) overlapped it.

The absolute yield at 125° is based on two runs. Other yield data at 125° had to be normalized to these runs because of an experimental difficulty discovered after the proportional-counter data were acquired. Seven data points were used for comparison. Data points taken from the angular distributions at $E_d = 6.66$, 7.29, and 7.93 MeV were also used for normalization. The average of 19 data points gave a normalization factor of 1.36 ± 0.16. After normalization there is an aver-

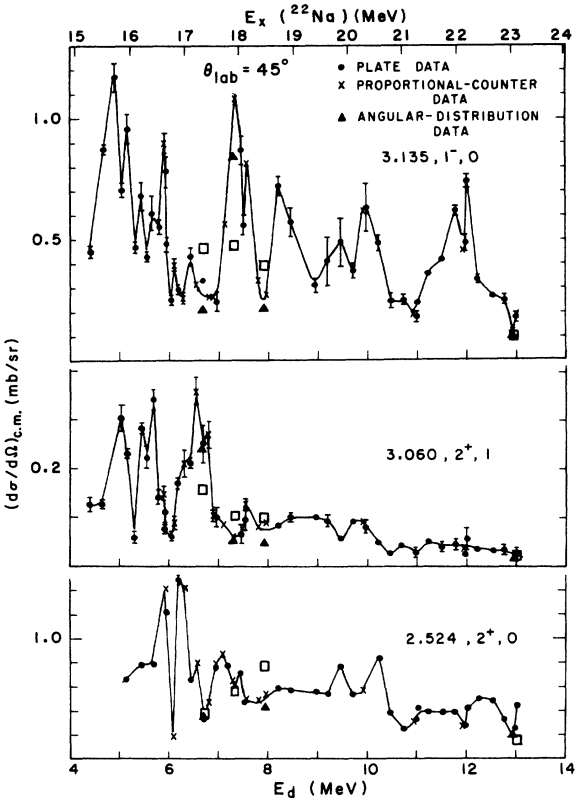

FIG. 4. Differential cross sections for ^{20}Ne$(d,\alpha)^{18}$F as a function of deuteron bombarding energy at a lab angle of 45° for the 2.524-, 3.060-, and 3.135-MeV states. Lines are drawn only to guide the eye. Squares show average cross sections from angular distributions and illustrate change in total cross section with energy.

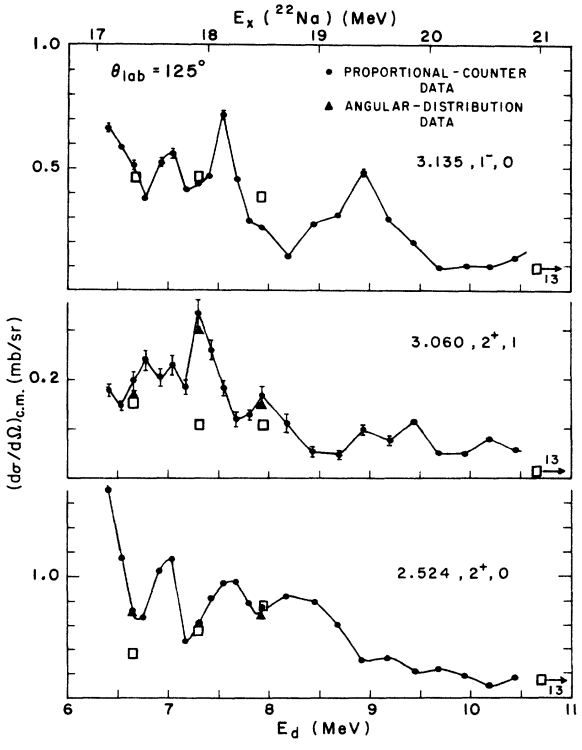

FIG. 5. Differential cross sections as a function of deuteron bombarding energy at a lab angle of 125° for the 2.524-, 3.060-, and 3.135-MeV states. Squares have the same meaning as those in Fig. 4.

age 10% difference between the yield and the angular-distribution data.

Angular Distributions

Angular distributions were taken at four deuteron energies, viz., 6.66, 7.29, 7.93, and 12.95 MeV for five states between 2.52 and 4.12 MeV excitation and the first three of these deuteron energies for the 2.101-MeV state. The three states at 3.72, 3.79, and 3.84 MeV were generally not well resolved and no angular distributions were extracted. From Figs. 4 and 5 we see that at 45° the cross section of the 3.060-MeV state peaks at about $E_d = 6.6$ MeV, has a valley at 7.29 MeV, and is flat near 13 MeV. In the 125° yield curve of Fig. 5, 6.66 MeV is on the side of a peak and 7.29 and 7.93 MeV are on peaks. Angular distributions were taken at these energies.

The $E_d = 6.66$-, 7.29-, and 7.93-MeV angular distributions were done in 10° steps except at selected forward and backward angles where 5° steps were taken, and the 12.95-MeV distribution was done in 20° steps. For all distributions, lab angles ranged from 15 to 135°. The forward limit is set by the gas-cell geometry and the backward limit by the angular range of the spectrograph.

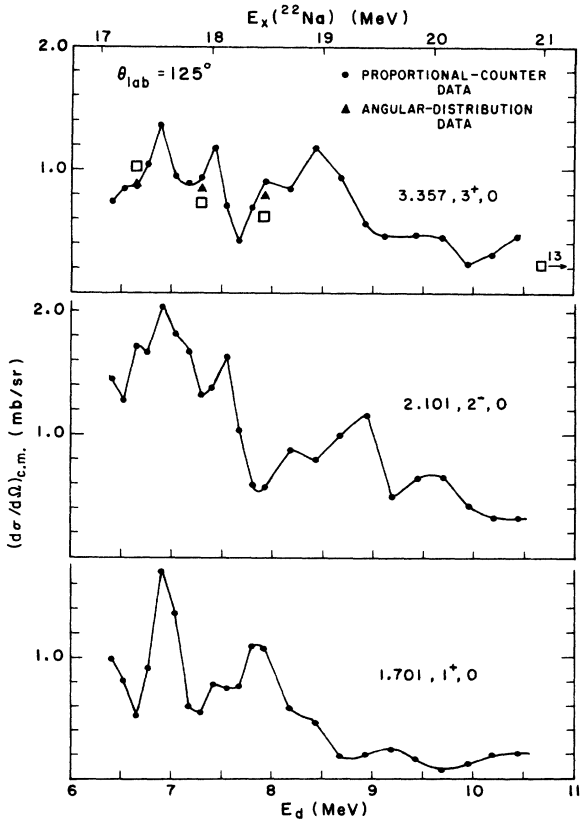

FIG. 6. Differential cross sections as a function of deuteron bombarding energy at a lab angle of 125° for the 1.701-, 2.101-, and 3.357-MeV states. Squares have the same meaning as those in Fig. 4.

All angular distributions were normalized to the 45° run using the monitor spectra from the −45 and −135° monitors. The distributions for the 2.1-MeV state contain less data than the others because for most runs this group was very near the end, or off the end, of the proportional counter. End effects in the counter make data for this state less reliable. Angular distributions for the two 2^+ states with $T = 0$ and $T = 1$, respectively, are shown in Fig. 7, whereas those for the other four states are given in Fig. 8.

In general, the angular distributions show neither backward nor forward peaking. It requires little imagination to call the angular distributions almost symmetric about 90° in the center of mass. There is one marked exception; the angular distribution at $E_d = 7.29$ MeV for the 3.060-MeV state is backward peaked. It should also be noticed that the 3.060-MeV angular distributions at $E_d = 7.93$ and 12.95 MeV are similar in shape, but the 12.95-MeV cross section is smaller by a factor of 5.6.

Since the ratio of the total cross sections was desired, the angular distributions were plotted as $(d\sigma/d\Omega)_{c.m.}$ versus $\cos\theta_{c.m.}$ and these curves were then integrated using a planimeter. Nearly the full angular range of cross section is covered by the data at forward angles ($\cos\theta_{c.m.} = 0.96$) but there is some significant amount of data lacking at the backward angles ($\cos\theta_{c.m.} = 0.8$).

A Legendre-polynomial fit was attempted for most of the angular distributions but we felt the fits were not very reliable. Usually the fits gave unphysical values for $d\sigma/d\Omega$ at 0 and/or 180°. The lack of backward-angle data appears to be the reason for the poor fits.

Table I shows the integrals between 15 and 125° lab, of the differential cross sections. If we assume that the differential cross sections over the unobserved 12% of the range of $\cos\theta$ have the same average value as over the observed range, the total cross sections are 1.14 times the values shown in Table I. The total cross sections so derived and then divided by 4π are plotted on the corresponding yield curves of Figs. 4, 5, and 6, using a square symbol. This illustrates the variation of total cross section with energy, especially the marked decrease at $E_d = 13$ MeV. Note that no yield curve was taken for the 4.119-MeV state and no cross section was obtained for the 1.701- and 2.101-MeV states.

Table II tabulates the ratio of the "total" cross section (values in Table I) for the 3.060-MeV,

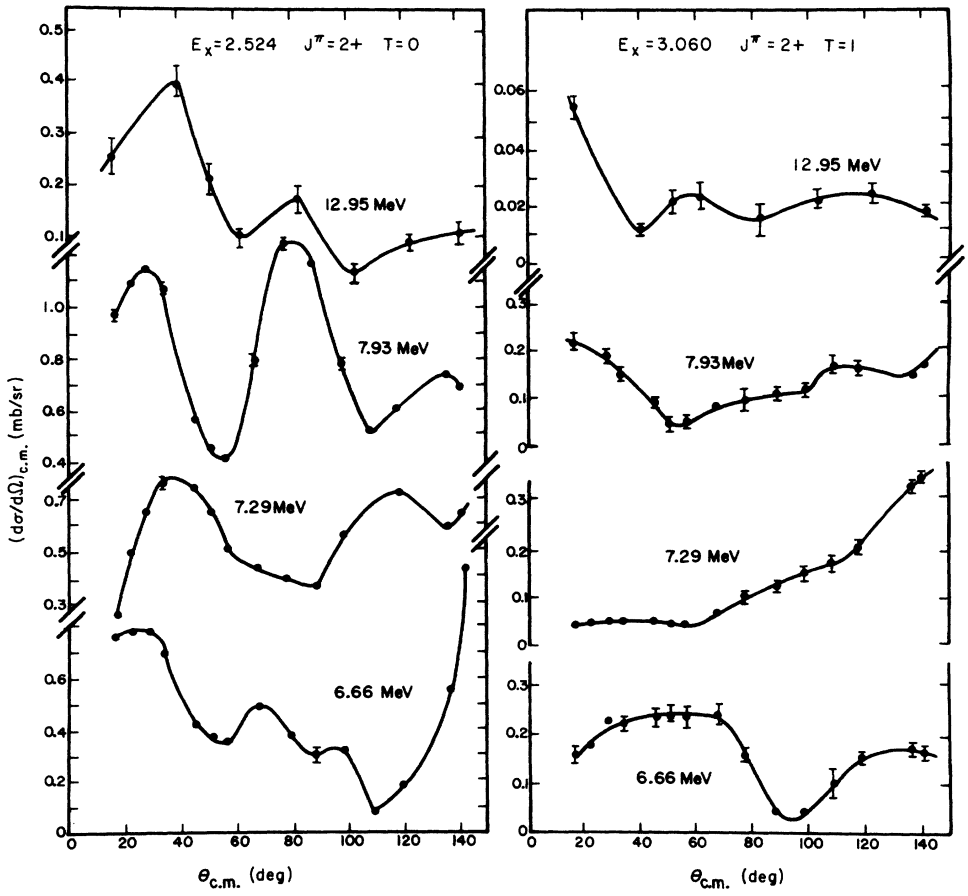

FIG. 7. Angular distributions for the ^{20}Ne$(d,\alpha)^{18}$F reaction at four input energies for the $J^\pi = 2^+$, $T = 0$, 1 states. Note that the distributions are displaced vertically and the ordinate scale is broken.

$J^\pi = 2^+$, $T = 1$ state to the other measured allowed states. Where the spins differ, the ratios were multiplied by $(2J+1)_{\text{allowed}}/(2J+1)_{\text{forbidden}}$ to correct for the statistical spin factors. Average values for the rows are shown on the right and, for the columns, at the bottom. In general the ratio decreases with increasing energy, but the ratio at 13 MeV is still 15% for the positive-parity states and 13% if we include the negative-parity state. These ratios reflect the amount of nonconservation of isospin. The over-all average of the intensity ratio is 21%. The range of this ratio for the four $T = 0$ states and the four energies is indicated by the standard deviation of 6.7% found for the over-all average.

TABLE I. Integral of differential cross sections between 15 and 125° lab angle (in mb). [a]

J^π; T	2^+; 0	2^+; 1	1^-; 0	3^+; 0	3^+; 0
E_x (MeV)	2.524	3.060	3.135	3.358	4.119
E_d (MeV)					
6.667	4.13 ± 0.06	1.74 ± 0.04	5.11 ± 0.05	11.39 ± 0.06	7.63 ± 0.06
7.293	6.16 ± 0.04	1.26 ± 0.03	5.19 ± 0.05	8.18 ± 0.04	7.46 ± 0.05
7.929	8.43 ± 0.05	1.23 ± 0.03	4.26 ± 0.11	6.96 ± 0.04	4.91 ± 0.05
12.950	1.65 ± 0.03	0.22 ± 0.018	1.05 ± 0.05	2.79 ± 0.03	1.53 ± 0.02

[a] The uncertainties in integrating the differential cross sections are shown. These do not include systematic errors in the differential cross sections themselves.

Uncertainties

The uncertainties in the differential cross sections measured with the proportional counter at 45° are primarily the random errors in the measured quantities. These are angle, G factor, temperature, pressure, charge, and number of counts. The total systematic uncertainty is indicated by the difference in the measured and accepted values of the p-p scattering cross section of 1.3%. Because of variations with energy and angle, the individual uncertainties do not combine simply, but estimates of accuracy obtained by adding random and systematic errors in quadrature are set at ±3.4% for all isolated states, ±5.7% for the 3.135-MeV state, and 5.7 to 20% for the 3.060-MeV state. Error bars are shown on the figures if they are larger than the point and represent only statistical and fitting errors. Because of the normalization required for the 125° data a 10% error is assigned to these yields.

Errors in the plate data are larger than those for the proportional-counter data because of the normalization and the possibility of an undetected contaminant. We estimate 10% uncertainty by comparing the normalized plate data with the proportional-counter data for nine overlapping data pairs.

The uncertainty in the "total" cross sections was estimated by taking equal intervals in $\cos\theta$ and adding in quadrature the error in each differential cross section times 2π, times the total region in $\cos\theta$, divided by $(N-1)$ data points. In addition to this uncertainty we have added in quadrature the error introduced by the planimeter. The uncertainties are shown in Table I and range from 0.5 to 8.2%. These uncertainties do not reflect systematic errors which affect all differential-cross-section measurements equally. The agreement with the p-p scattering results suggests that these are less than 2%. We estimated the uncertainty in total cross-section ratios by adding in quadrature the errors in the total cross sections to be compared. The uncertainty in these ratios, which are given in Table II, range from 2.4 to 9.4%.

IV. DISCUSSION

The resonant character of the yield curves coupled with the nearly symmetric angular distributions, strongly suggests that the ^{20}Ne$(d, \alpha)^{18}$F reaction proceeds via the compound nucleus ^{22}Na in the energy range investigated. This symmetry is emphasized by the angular distributions summed over final states which are plotted for the lowest and highest energy distributions in Fig. 9. The excitation region of 15 to 23 MeV in ^{22}Na covered by this experiment has not been extensively studied, but one expects a fairly high level density so the average spacing (D^J) of levels with spin and parity J^π should be less than the Coulomb matrix element $\langle H_C \rangle$ and the static criterion for isospin conservation will not hold. One then asks whether the dynamic criterion $\langle \Gamma \rangle \gg \langle H_C \rangle$ applies. Now from the plot given by Jänecke *et al.*[7] we estimate $\langle \Gamma \rangle = 75$ keV for 15 MeV excitation in ^{22}Na and 150 keV for 23 MeV excitation. It has been estimated[26, 27] that $\langle H_C \rangle$ is of the order of 100 keV although a recent measurement by Braithwaite *et al.*[28] on ^{12}C* indicates an $\langle H_C \rangle$ of about 250 keV in that case. Thus at the lower end of our energy range $\langle \Gamma \rangle$ certainly is not greater than $\langle H_C \rangle$ and we expect a significant violation of isospin conservation. At the upper end of the range $\langle \Gamma \rangle$ is greater than or comparable to $\langle H_C \rangle$ and the violation should begin to decrease. Also, Wilkinson[26] estimates that the region of large nonconservation of isospin, where D^J approaches $\langle H_C \rangle$ but before $\langle \Gamma \rangle > \langle H_C \rangle$, has a lower limit of 6 to 10 MeV ex-

TABLE II. Ratio of total cross section[a] of $T=1$ state to total cross section of four $T=0$ states.[b]

	$\frac{\sigma(3.060)}{\sigma(2.524)} \times 1$	Percent error	$\frac{\sigma(3.060)}{\sigma(3.135)} \times \frac{3}{5}$	Percent error	$\frac{\sigma(3.060)}{\sigma(3.358)} \times \frac{7}{5}$	Percent error	$\frac{\sigma(3.060)}{\sigma(4.119)} \times \frac{7}{5}$	Percent error	Average
E_d (MeV)									
6.667	0.420	2.9	0.204	2.6	0.213	2.5	0.319	2.6	0.289
7.293	0.205	2.4	0.146	2.5	0.215	2.4	0.237	2.4	0.201
7.929	0.146	3.0	0.172	3.9	0.247	3.0	0.350	3.0	0.229
12.950	0.133	8.4	0.063	9.4	0.110	8.3	0.201	8.3	0.127
Average	0.226		0.146		0.196		0.277		0.212

[a] Values are the ratio of the integral of the differential cross sections measured between 15 and 125° lab, multiplied by the factor $(2J_1+1)/(2J_2+1)$.

[b] Column headings designate the cross sections with the excitation energies of the two states and show the multiplying factor.

citation and an upper limit of 14 to 18 MeV for light $4n+2$ nuclei. Table II shows that at the upper end of our energy range the expected decrease does in fact occur. At $E_d = 12.95$ MeV the ratio of forbidden to allowed cross sections, averaged for four allowed states, is 12.7% compared to 20 to 29% at the lower energies. The ratio to the allowed 2^+ state drops from 42% at $E_d = 6.66$ MeV to 13.3% at 12.95 MeV. The magnitude of the violation which averages $21.2 \pm 6.7\%$ and goes as high as 40% is, however, considerably larger than those seen with other (d, α) reactions.

Of the (d, α) reactions studied to data only a very few are not between 0^+ initial and 0^+ final states. One of these is $^{14}N(d, \alpha)^{12}C$ investigated by Browne, Schier, and Wright[29] which proceeds from a 1^+ initial state. Two $T=1$ final states were observed: the 15.11 MeV, $J^\pi = 1^+$, $T=1$ and the 16.11, 2^+, 1. The ratio of the intensities to the 12.71, 1^+, 0 state at 7.18-MeV bombarding energy was only 3% and was attributed to compound-nucleus mixing. The $^{10}B(d, \alpha)^8Be$ reaction, investigated most recently by Callender and Browne,[4] showed nearly equal population of the final 2^+ states at 16.6 and 16.9 MeV. In the same reaction, however, the $J=1^+$ states at 17.6 and 18.15 MeV showed quite unequal population. The ratio of the 17.64-MeV ($T=1$) state to the 18.15-MeV ($T=0$) state lay between 9 and 12% at selected energies and angles between 8 and 12 MeV. At present these are the only two examples of isospin-nonconserving (d, α) reactions between other than a 0^+ initial state and a 0^+ final state. Some preliminary data[30] on the $^{32}S(d, \alpha)^{30}P$ reaction, between 6 and 7 MeV at 30° lab angle, to the 2.94-MeV, $J^\pi = 2^+$, $T=1$ state indicate yields comparable to allowed-state yields. Endt and Paris[31] also found the average intensities from this reaction to four $T=1$ states in ^{30}P to be 50% of neighboring $T=0$ states for two bombarding energies and three observation angles.

So in these reactions where angular momentum is not an important factor there are three examples; $^{12}C(15.11)$, $^{12}C(16.11)$, and $^8Be(17.64)$; where $T=1$ states are not strongly excited and one example of equal excitation; ^8Be (16.6 and 16.9). The case of $^{20}Ne(d, \alpha)^{18}F$ seems to lie in between the two extremes. The $T=1$ cross section is high (20 to 40% of allowed states) compared to the other three cases but the cross section and group shapes do not indicate complete mixing as in ^8Be. Groups leading to the other $T=1$ states of ^{18}F in the 4-MeV region of excitation are present in only our plate data but it appears that these three states are significantly excited.

Let us now further consider initial- and final-

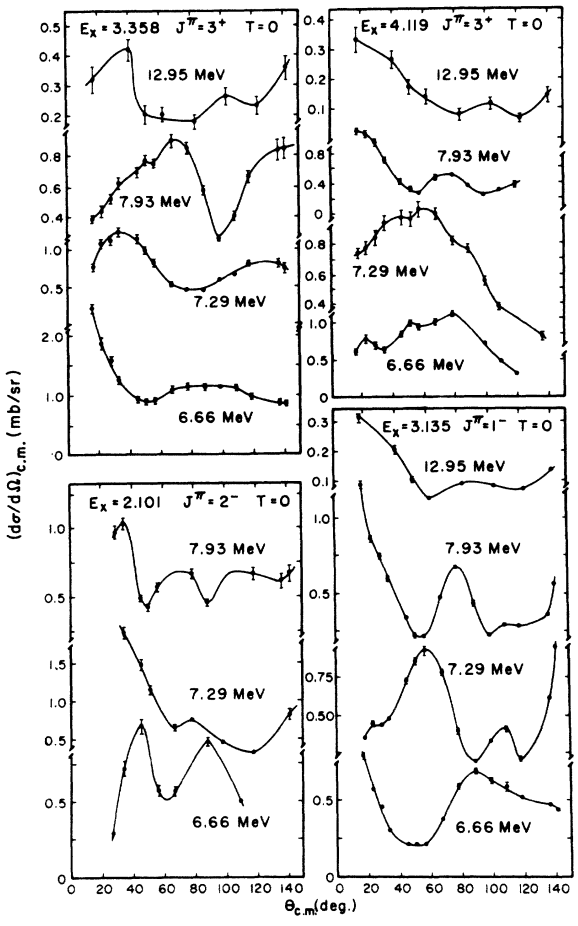

FIG. 8. Angular distributions for four $T=0$ states in ^{18}F. Note that the distributions are displaced vertically and the ordinate scale is broken.

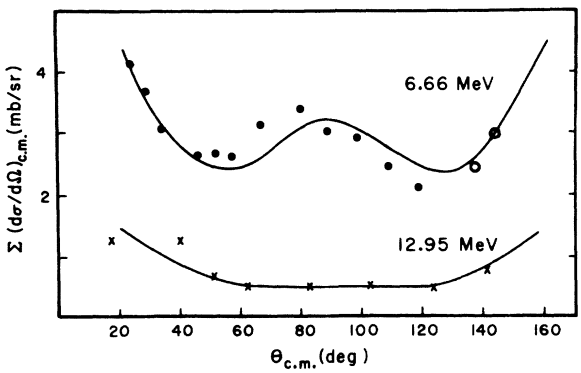

FIG. 9. Sum of angular distributions of the 2.524-, 3.061-, 3.135-, 3.358-, and 4.119-MeV states for the lowest and highest bombarding energies at which distributions were taken. The open circles indicate that the cross section of the 4.119-MeV state had to be estimated at these angles.

state impurities. Theoretical predictions of the isospin purity of the ground states of the initial nuclei in question are a few tenths of a percent,[27] so initial-state mixing should not contribute significantly. For all observed isospin-nonconserving reactions to 0^+ ($T=1$) final states, the next nearest 0^+ ($T=0$) final state is several MeV (4 to 15) away and MacDonald's estimates of a few tenths of a percent should apply to the observed $T=1$ states.[27] In the case of ^{12}C final states, the $T=1$ state is at 15.1 MeV and the next nearest 1^+, $T=0$ state is at 12.7 MeV, a separation of 2.4 MeV. In this case the final-state mixing estimate used above gives $I=0.002$. Even using the value for $\langle H_C \rangle$ given by Braithwaite *et al.* one gets only 0.01. Therefore in all other reactions which have been studied, except ^{10}B(d, α)-^{8}Be, one expects the contribution from impurity of the final states to be very small.

For our ^{20}Ne(d, α)^{18}F reactions, however, the nearest $J^\pi = 2^+$, $T=0$ states are at 2.524 and 3.836 MeV, which are 536 and 776 keV, respectively, from the 3.060, 2^+, 1 state. The amplitude for mixing (a_v) is $H_C/\Delta E$, where ΔE is the energy difference between states of the same spin and parity but different isospin.[26] For $\langle H_C \rangle = 100$ keV, $a_{3.84} = 0.129$ and $a_{2.52} = 0.171$. To calculate the intensity one sums over all interacting pairs of levels of the same spin and parity. The two nearest 2^+ states contribute most to the sum and then $I = \sum a_v^2 = 0.05$. If $\langle H_C \rangle$ is appreciably larger than 100 keV the final state may be much less pure $T=1$, e.g. for $\langle H_C \rangle = 250$ keV the mixing of the 3.836-MeV state alone would give $I=0.10$. Final-state impurity could easily account for a violation of 5 to 15% in this reaction.

It seems probable that the combination of 5% or more final-state mixing with compound-nuclear mixing accounts for the large forbidden-to-allowed ratios observed. The 13% found at 13 MeV may arise largely from final-state impurity and the compound-nuclear mixing may have become small. On the other hand a larger $\langle H_C \rangle$ would imply that still higher input energies would be required to make compound-nuclear mixing negligible. It would be desirable to extend the energy range, if experimental difficulties can be overcome. Although this experiment does not rule out some direct process (as suggested by Noble and others[32]), the data show nothing to indicate a direct process in the energy range studied.

V. SUMMARY

An isospin selection-rule violation of the order of 20% was established for the second $T=1$ state in ^{18}F in the ^{20}Ne(d, α)^{18}F reaction at four energies from 6.6 to 13 MeV. In the lower region of input deuteron energies the reaction proceeds via the compound nucleus. At the upper end of the region (13 MeV) the compound-nuclear mixing appears to decrease. The major portion of the observed violation is caused by Coulomb mixing in the compound nucleus, but comparisons of these data with other (d, α) reactions suggest that considerable final-state mixing also contributes.

---

*Work supported by the National Science Foundation under Grant No. GP-27456. It is based on a dissertation submitted by A. F. Hrejsa to the Graduate School of the University of Notre Dame in partial fulfillment of the requirements for the Ph.D. degree.

†Present address: M. D. Anderson Hospital, Houston, Texas.

[1]For a summary up to 1966 see C. P. Browne, in *Isobaric Spin in Nuclear Physics*, edited by J. D. Fox and D. Robson (Academic, New York, 1966), pp. 136—161.

[2]J. W. Hemsky, E. Bleuler, and D. J. Tendam, Nucl. Phys. A105, 665 (1967).

[3]J. Jobst, S. Messelt, and H. T. Richards, Phys. Rev. 178, 1663 (1969).

[4]W. D. Callender and C. P. Browne, Phys. Rev. C 2, 1 (1970), and references cited therein.

[5]A. Richter, L. Meyer-Schützmeister, and J. C. Stoltzfus, Phys. Rev. C 2, 1361 (1970).

[6]P. Jolivette, Ph.D. thesis, University of Wisconsin, 1970 (unpublished). Available through University Microfilms Inc., Ann Arbor, Michigan.

[7]J. Jänecke, T. F. Yang, W. S. Gray, and R. M. Polichar, Phys. Rev. C 3, 79 (1971).

[8]L. Meyer-Schützmeister, D. von Ehrenstein, and R. G. Allas, Phys. Rev. 147, 743 (1966); D. von Ehrenstein, L. Meyer-Schützmeister, J. E. Monahan, A. Richter, and J. C. Stoltzfus, Phys. Rev. Lett. 27, 107 (1971).

[9]H. T. Richards and H. V. Smith, Jr., Phys. Rev. Lett. 27, 1735 (1971); H. V. Smith, Jr., Phys. Rev. C 6, 441 (1972).

[10]G. M. Matous and C. P. Browne, Phys. Rev. 136, B399 (1964).

[11]F. C. Barker, Nucl. Phys. 83, 418 (1966).

[12]P. R. Chagnon, Nucl. Phys. 78, 193 (1966); A. R. Poletti, and E. K. Warburton, Phys. Rev. 137, B595(1965).

[13]F. Ajzenberg-Selove, Nucl. Phys. A190, 1 (1972).

[14]Y. Hashimoto and W. P. Alford, Phys. Rev. 116, 981 (1959).

[15]P. L. Jolivette, H. Stocker, and A. F. Hrejsa, Bull. Am. Phys. Soc. 16, 1171 (1971).

[16]M. A. Spivak, Rev. Sci. Instrum. 41, 1614 (1970). Parylene is made by Chemical and Plastics Division of Union Carbide, Bound Brook, New Jersey.

[17]Supplied by Chromium Corporation of America.

[18]Supplied by CVC Bendix Corporation.

[19]A. F. Hrejsa, Ph.D. thesis, University of Notre Dame,

1972 (unpublished).
[20]Supplied by Mound Laboratories of Union Carbide Corporation.
[21]R. J. Slobodrian, H. E. Conzett, E. Shield, and W. F. Tivol, Phys. Rev. 174, 1122 (1968).
[22]J. B. Marion and A. S. Ginzbarg, AEC Report No. NP-6241, 1959 (unpublished) (Office of Technical Services, Department of Commerce, Washington, D. C.).
[23]E. Silverstein, Nucl. Instrum. Methods 4, 53 (1959).
[24]W. C. Davidon, Argonne National Laboratory Report No. ANL-5990 (Rev. 2), Feb. 1966 (unpublished).
[25]F. C. Young, B. Cotton, and R. A. Lindgren, Bull. Am. Phys. Soc. 16, 1154 (1971).
[26]D. H. Wilkinson, Philos. Mag. 1, 379 (1956).
[27]W. M. MacDonald, in *Nuclear Spectroscopy* edited by F. Ajzenberg-Selove (Academic, New York, 1960), Part B, pp. 932–959.
[28]W. J. Braithwaite, J. E. Bussolette, F. E. Cecil, and G. T. Garvey, Phys. Rev. Lett. 29, 276 (1972).
[29]C. P. Browne, W. A. Schier, and I. F. Wright, Nucl. Phys. 66, 49 (1965).
[30]N. Detorie, J. Goss, H. Stocker, and A. A. Rollefson, private communication.
[31]P. M. Endt and C. H. Paris, Phys. Rev. 110, 89 (1958).
[32]J. V. Noble, Phys. Rev. 162, 934 (1967); Phys. Rev. Lett. 22, 473 (1969); R. J. Drachman, Phys. Rev. Lett. 17, 1017 (1966); T. A. Griffy, Phys. Rev. Lett. 21, 693 (1966); R. G. Clarkson and T. A. Griffy, Bull. Am. Phys. Soc. 12, 207 (1967).